Supplement of Atmos. Chem. Phys., 24, 5315–5335, 2024
https://doi.org/10.5194/acp-24-5315-2024-supplement

Atmospheric Chemistry and Physics
Open Access
EGU

Supplement of

Potential of using CO_2 observations over India in a regional carbon budget estimation by improving the modelling system

Vishnu Thilakan et al.

Correspondence to: Dhanyalekshmi Pillai (dhanya@iiserb.ac.in)

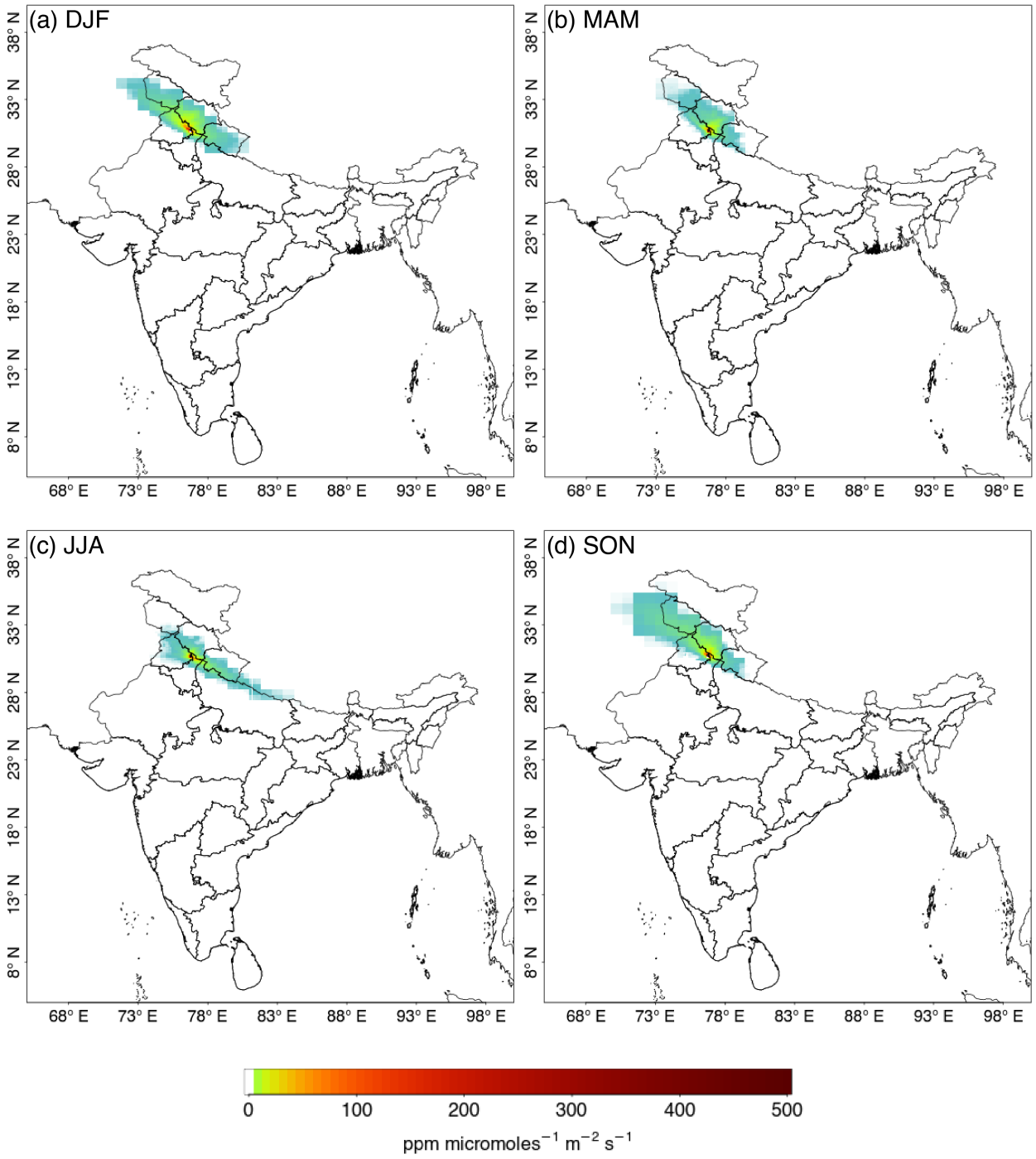

Figure S1. Seasonally integrated STILT footprints for Mohali during 2017. (a) Winter (b) Pre-Monsoon (c) Monsoon (d) Post-Monsoon

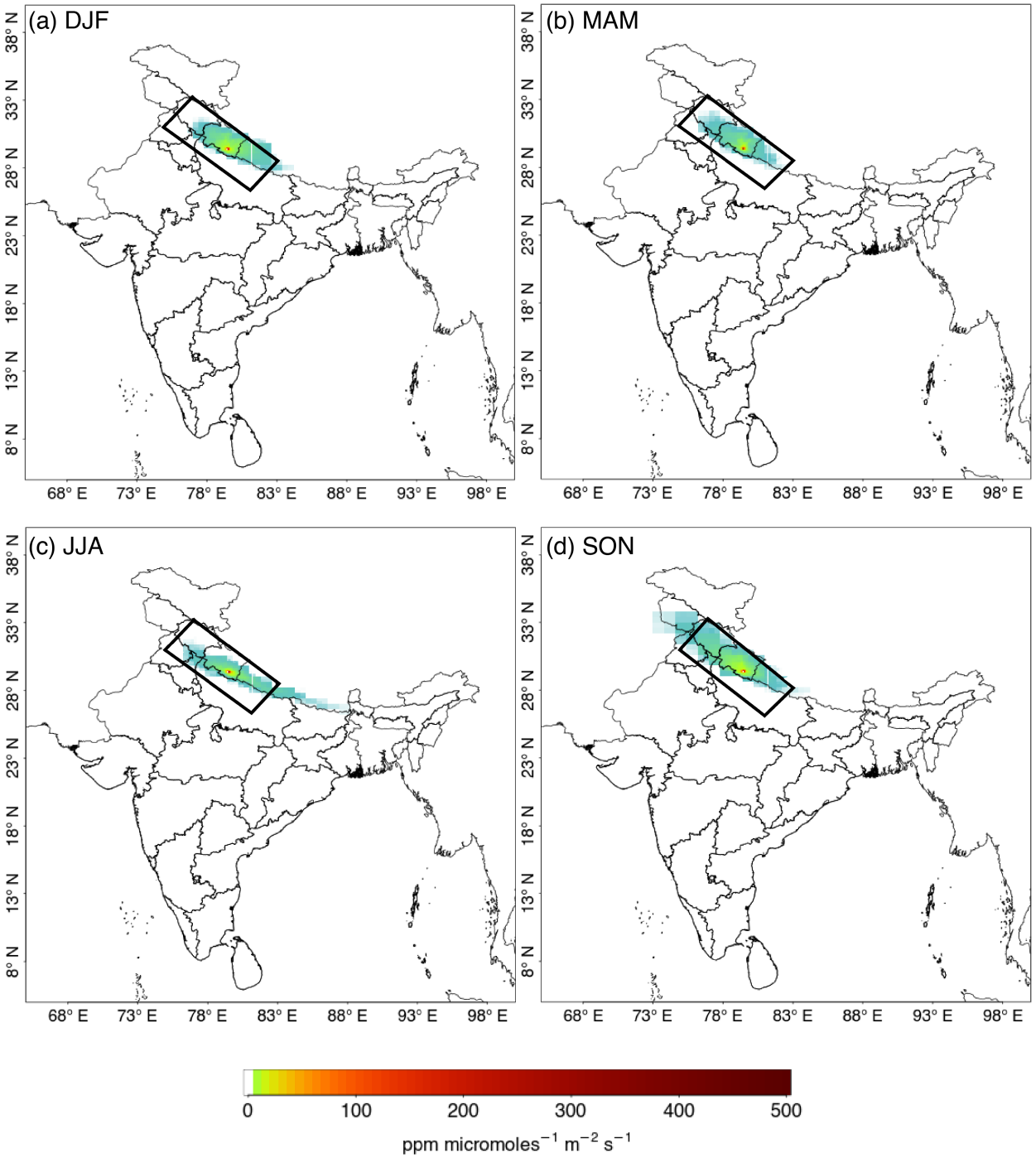

Figure S2. Seasonally integrated STILT footprints for Nainital during 2017. The marked region represents the area used for the MODIS NDVI analysis. (a) Winter (b) Pre-Monsoon (c) Monsoon (d) Post-Monsoon

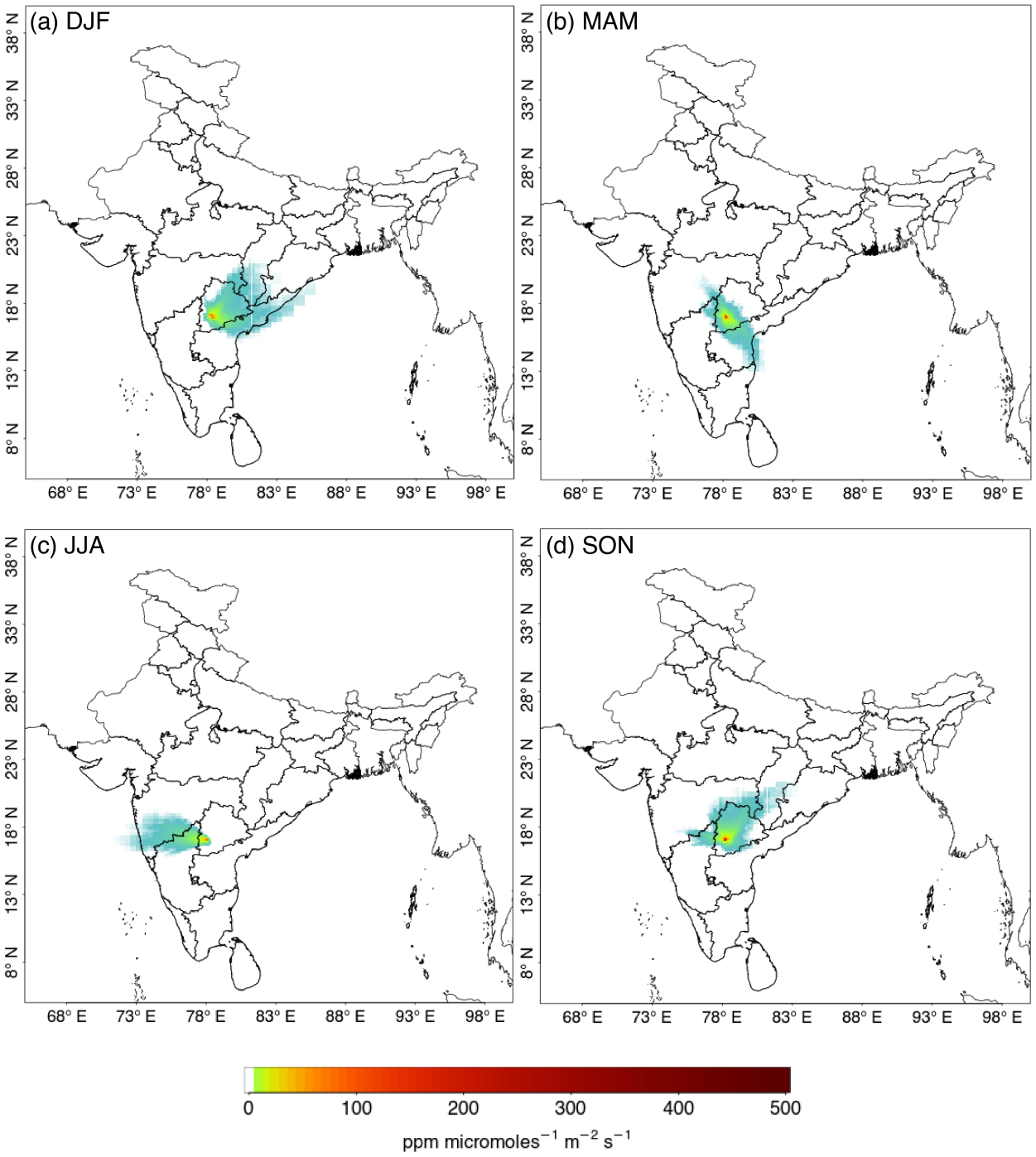

Figure S3. Seasonally integrated STILT footprints for Shadnagar during 2017. (a) Winter (b) Pre-Monsoon (c) Monsoon (d) Post-Monsoon

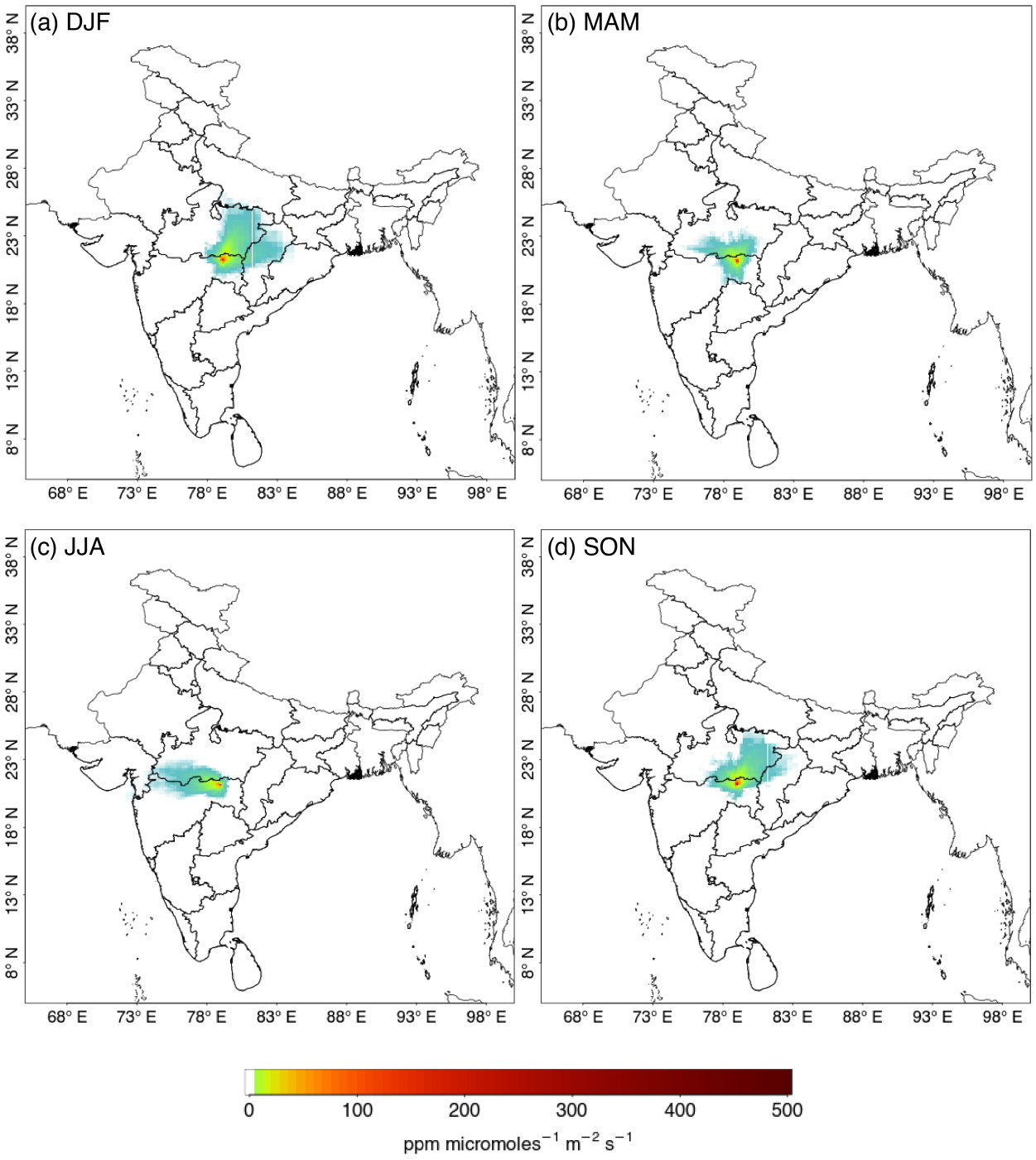

Figure S4. Seasonally integrated STILT footprints for Nagpur during 2017. (a) Winter (b) Pre-Monsoon (c) Monsoon (d) Post-Monsoon

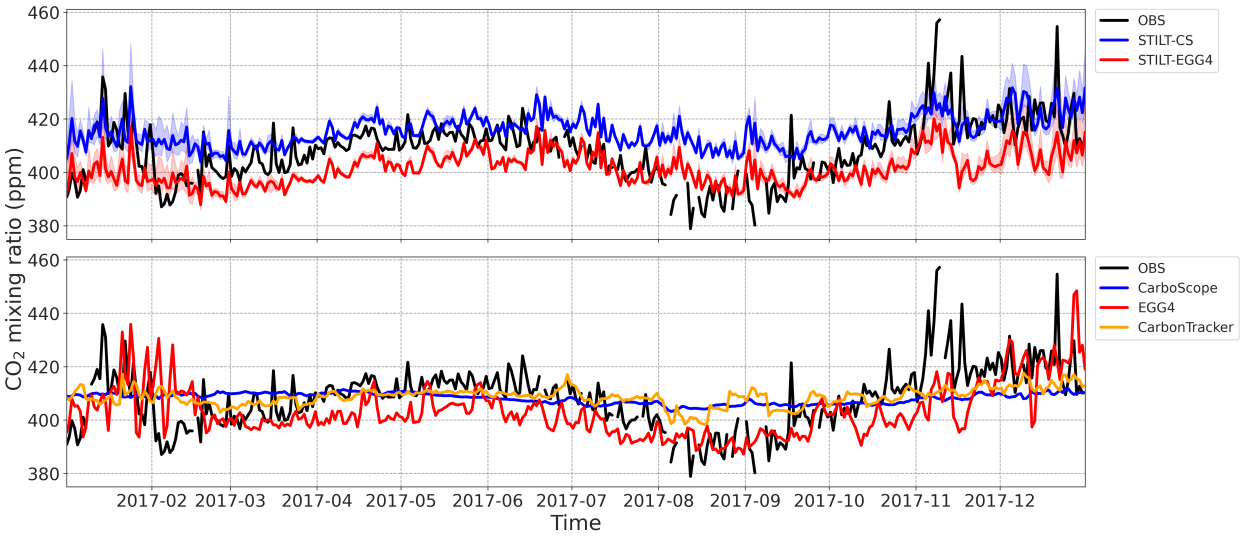

Figure S5. CO_2 daytime (11:00-16:00 local time) average time series from Mohali during 2017 with (a) STILT simulations. Blue (STILT-CS) and red (STILT-EGG4) curves represent the ensemble average of the STILT simulations using different anthropogenic fluxes. Shaded regions represent the range of the model simulations. (b) Global reanalysis products.

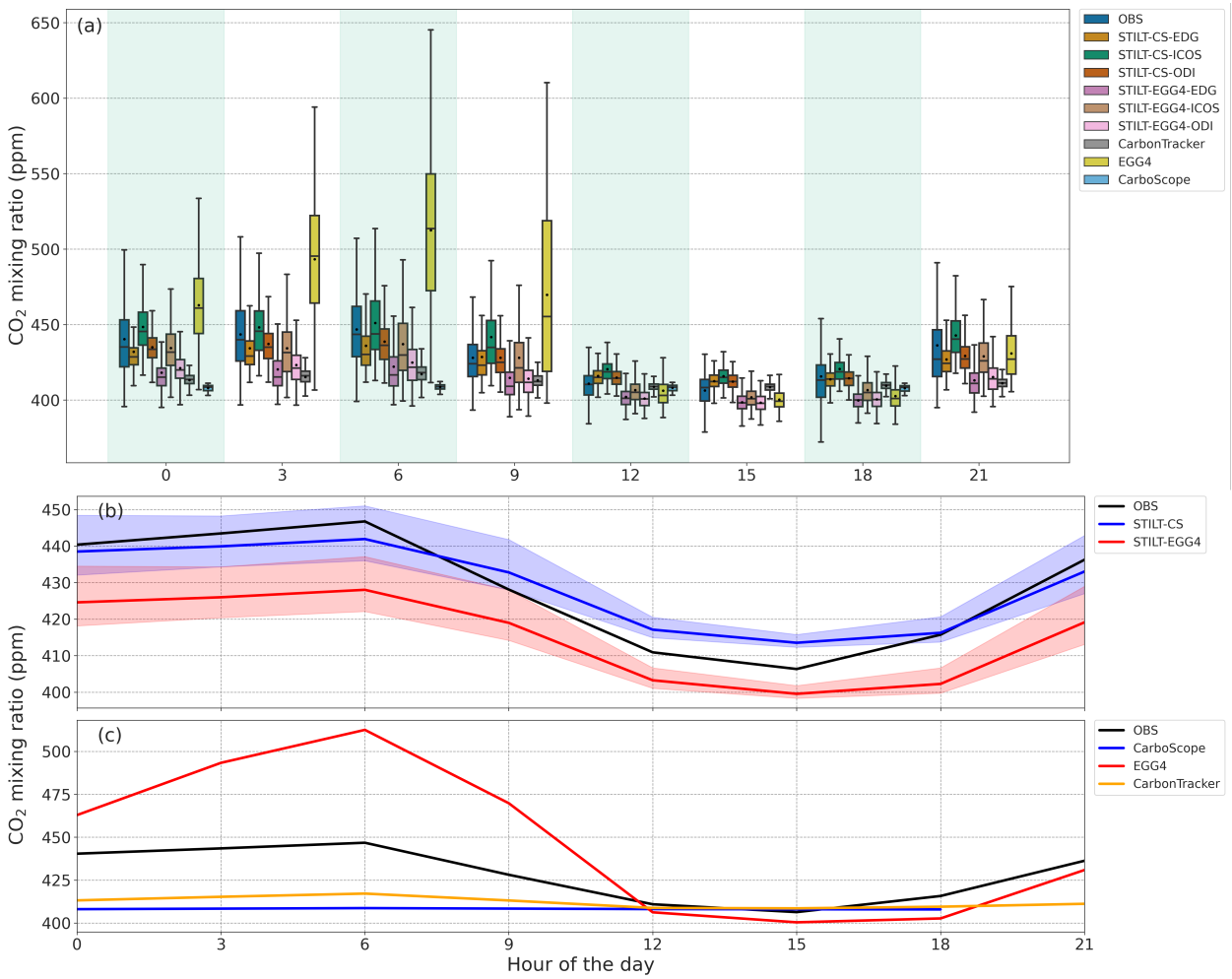

Figure S6. Diurnal variability in CO_2 concentration over Mohali during 2017. (a) Box and whisker plot of observation in comparison with model simulations is shown. The box denotes the interquartile range, and the whiskers represent the points within 1.5 times the interquartile range from the lower and upper quartile. Additionally, mean values for the CO_2 concentration are provided as a black circle inside the box (b) Time series of CO_2 diurnal cycle is shown in comparison with STILT simulations. Blue (STILT-CS) and red (STILT-EGG4) curves represent the ensemble average of the STILT simulations using different anthropogenic fluxes. Shaded regions represent the range of the model simulations. (c) Comparison of CO_2 diurnal cycle with global reanalysis products. Note that STILT provides output only every three hours. Similarly, EGG4 and CarbonTracker provide outputs at a three-hour resolution and CarboScope at a six-hour resolution.

Figure S7. CO_2 diurnal cycle over Mohali for different seasons during 2017 is shown in comparison with STILT-CS simulations, STILT-EGG4 simulations and global reanalysis products. Note that STILT provides output only every three hours. Box and whisker plot of observation in comparison with model simulations is given for (a) Winter, (b) Pre-Monsoon, (c) Monsoon and (d) Post-Monsoon seasons. The box denotes the interquartile range, and the whiskers represent the points within 1.5 times the interquartile range from the lower and upper quartile. Additionally, mean values for the CO_2 concentration are provided as a black circle inside the box. Similarly, EGG4 and CarbonTracker provide outputs at a three-hour resolution and CarboScope at a six-hour resolution.

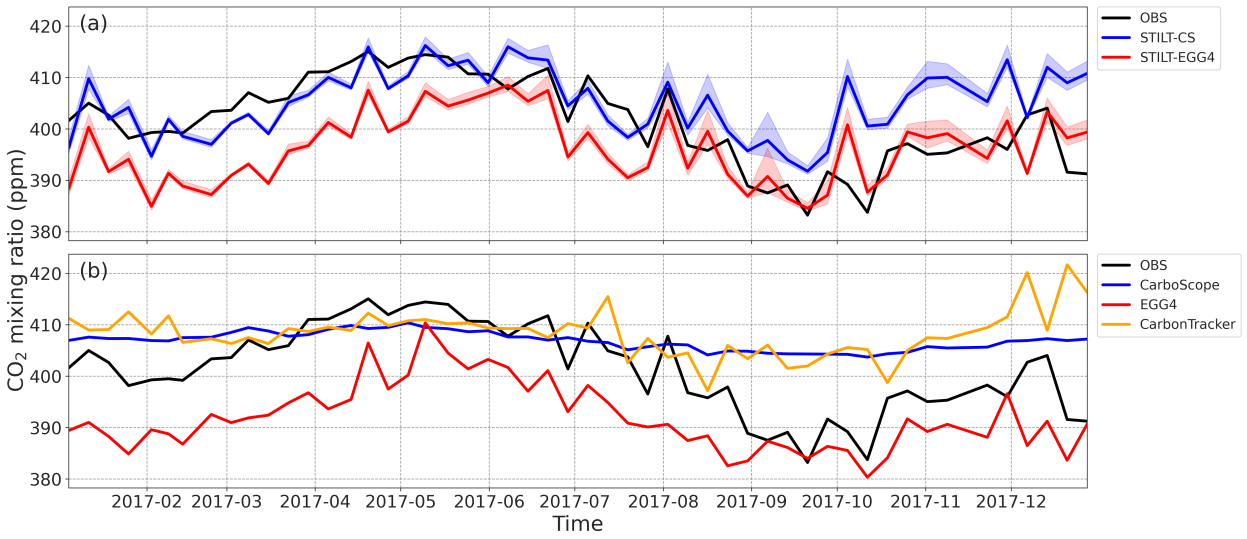

Figure S8. CO_2 time series of weekly observations (14:00 local time) at Nainital during 2017 with (a) STILT simulations. Blue (STILT-CS) and red (STILT-EGG4) curves represent the ensemble average of the STILT simulations using different anthropogenic fluxes. Shaded regions represent the range of the model simulations. (b) Global reanalysis products.

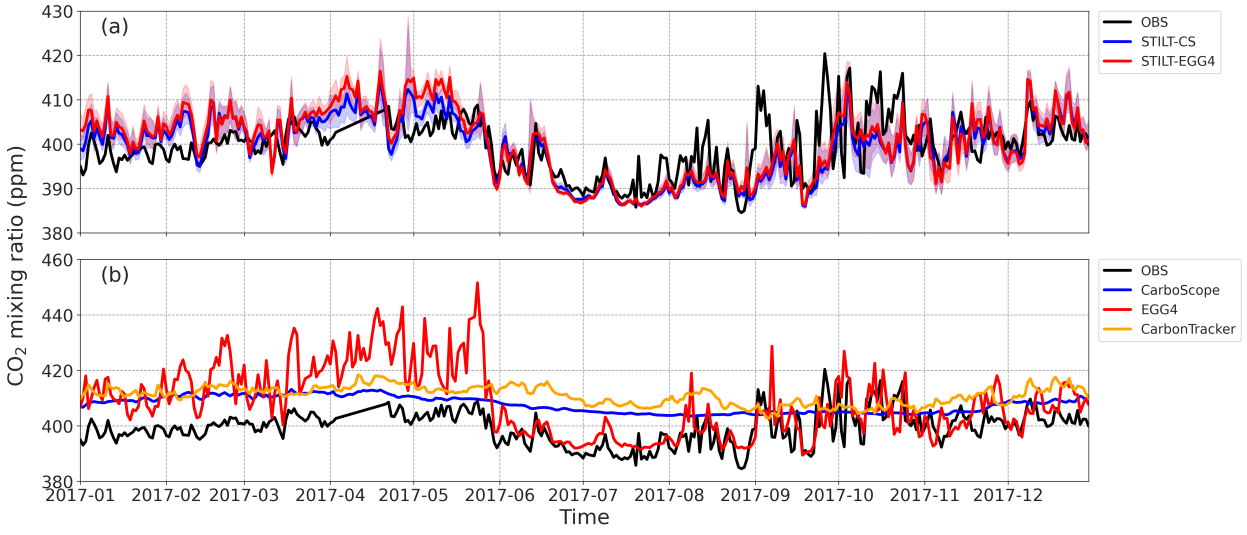

Figure S9. CO_2 daily mean time series from Shadnagar during 2017 with (a) STILT simulations. Blue (STILT-CS) and red (STILT-EGG4) curves represent the ensemble average of the STILT simulations using different anthropogenic fluxes. Shaded regions represent the range of the model simulations. (b) Global reanalysis products.

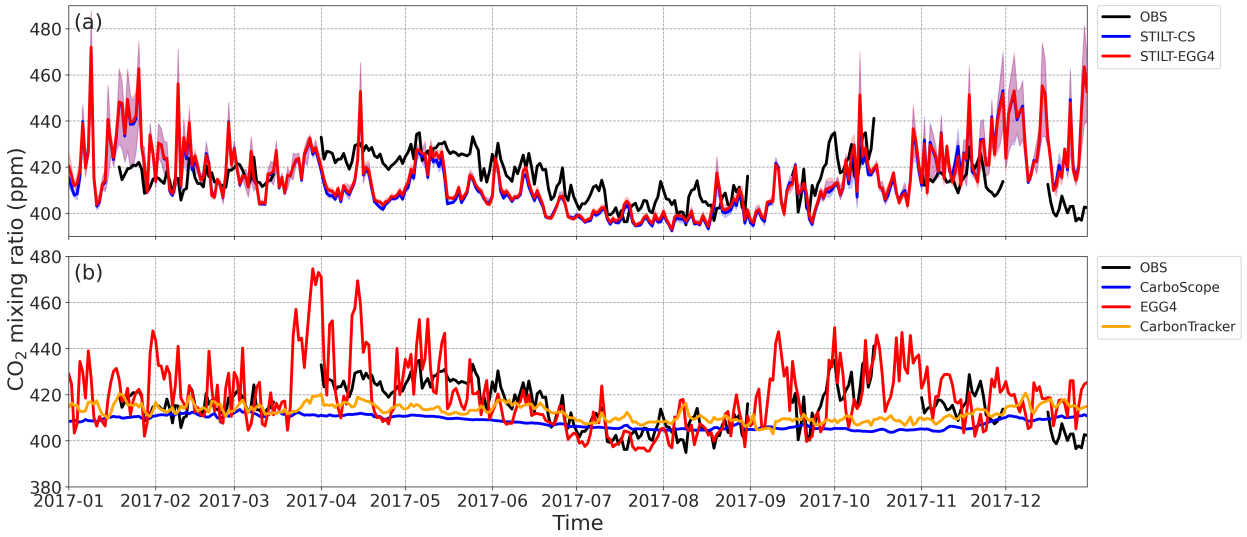

Figure S10. CO_2 daily mean time series from Nagpur during 2017 with (a) STILT simulations. Blue (STILT-CS) and red (STILT-EGG4) curves represent the ensemble average of the STILT simulations using different anthropogenic fluxes. Shaded regions represent the range of the model simulations. (b) Global reanalysis products.

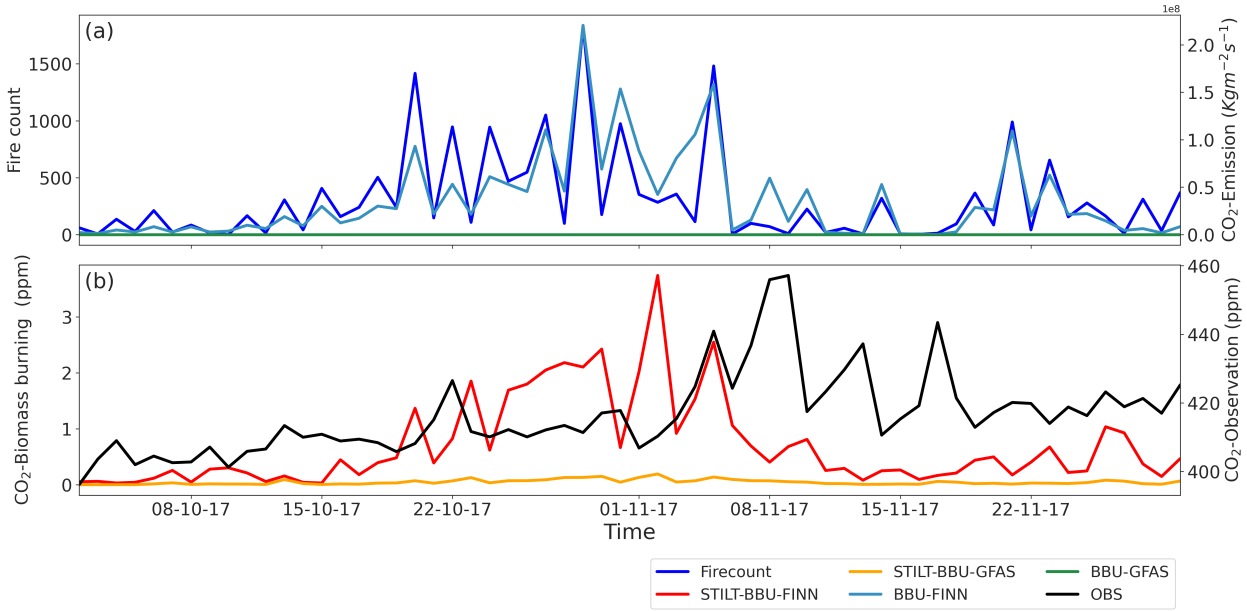

Figure S11. Biomass burning over Mohali footprint region during October-November 2017. (a) Time series of MODIS fire counts over Mohali influence region (see Fig. S1) during October-November 2017. (b) Time series of CO_2 daytime observations over Mohali in comparison with the CO_2 biomass burning components from STILT simulations. The black line represents CO_2 daytime observations, the red line corresponds to the CO_2 biomass burning component from STILT-FINN, and the orange line corresponds to CO_2 biomass burning component from STILT-GFAS (see Sect. 6.1).

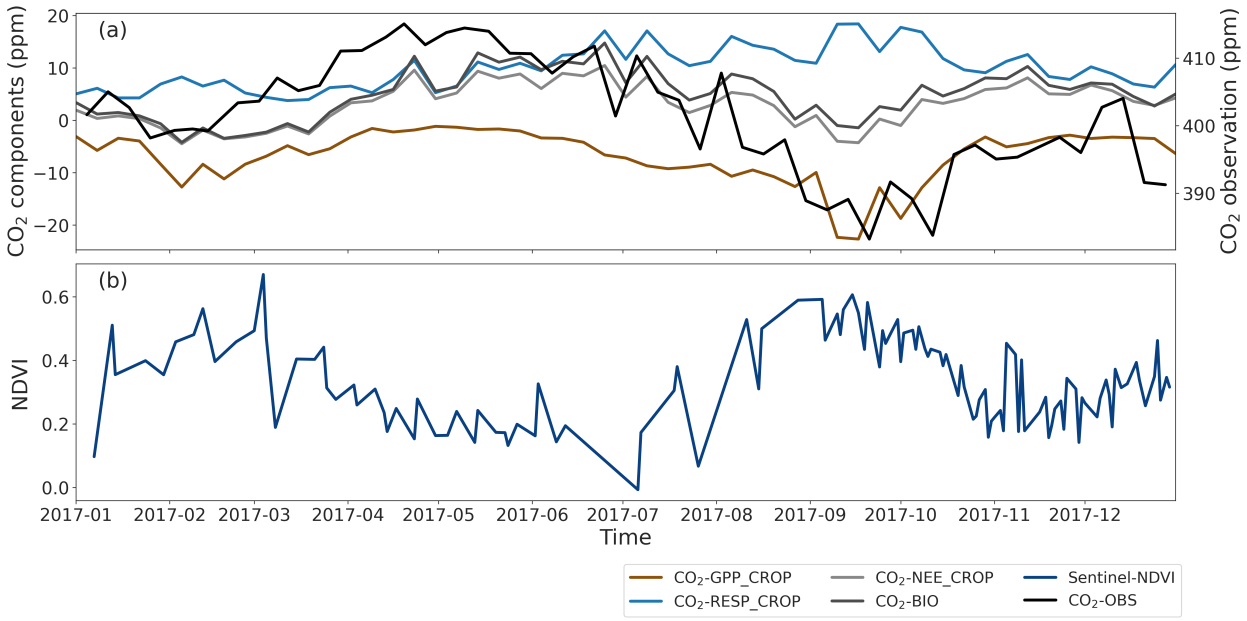

Figure S12. CO_2 variability over Nainital in association with crop production. CO_2 observation is shown in comparison with (a) CO_2 biospheric components from STILT simulations. (b) NDVI estimation using Sentinel-2 data over Nainital influence region (see Fig. S2) during 2017.

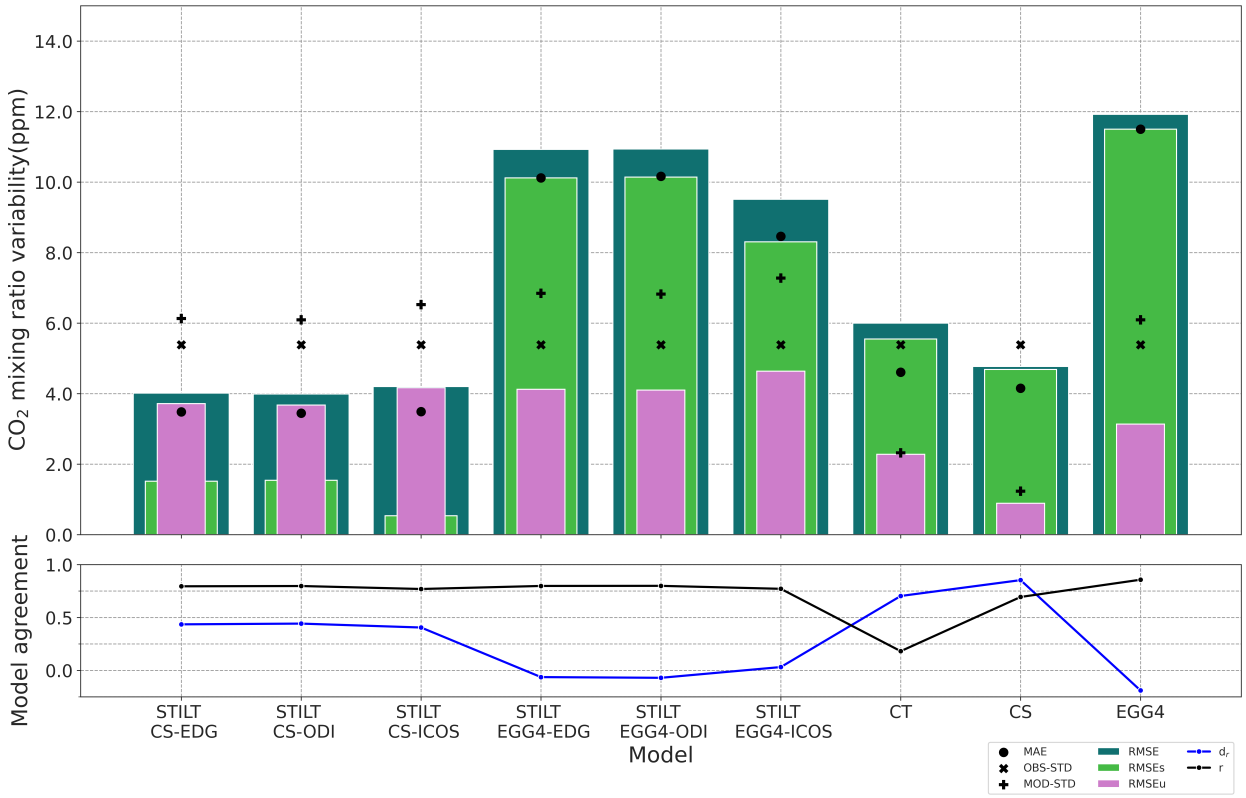

Figure S13. An overview of the performance of models (see Sect. 4) at Nainital for the period January to July. Bar plots represent the different RMSE (in teal), systematic RMSE ($RMSE_s$, in lime green) and unsystematic RMSE ($RMSE_u$, in orchid) values estimated for each station. MAE (•), observed standard deviation (×) and model standard deviation (+) are overlied on barplots. The blue and black lines represent the index of agreement (d_r) and correlation coefficient (r) values, respectively.